L- and M-Cone–Driven Electroretinograms in Stargardt's Macular Dystrophy–Fundus Flavimaculatus

Hendrik P. N. Scholl,[1] *Jan Kremers,*[1] *Reinhard Vonthein,*[2] *Karen White,*[3] *and Bernhard H. F. Weber*[3]

Purpose. To study the dynamics of the long (L)- and middle (M)-wavelength–sensitive cone-driven pathways and their interactions in patients with Stargardt's macular dystrophy-fundus flavimaculatus (SMD-FF) and to correlate them with other clinical parameters and individual genotypes.

Methods. Forty-seven patients with SMD-FF participated in the study. In addition to standard 30-Hz flicker electroretinograms (30-Hz fERG), ERG responses were measured to stimuli that modulated exclusively the L or the M cones (L/M cones) or the two simultaneously. Blood samples were screened for mutations in the 50 exons of the *ABCA4* gene.

Results. Patients with SMD-FF did not show a decrease in the mean L/M-cone–driven ERG sensitivity, but there was a significant increase in the interindividual variability. The mean L-/M-cone weighting ratio was normal. However, the L-cone–driven ERG was significantly phase delayed, whereas the M-cone–driven ERG was significantly phase advanced. These phase changes were significantly correlated with disease duration. The amplitude and implicit time of the standard 30-Hz fERG both correlated significantly with the L/M-cone–driven ERG sensitivity and with the phase difference between the L/M-cone–driven ERGs, indicating the complex origin of the standard 30-Hz fERG. Probable disease-associated mutations in the *ABCA4* gene were found in 40 of 45 patients, suggesting that they form a genetically fairly uniform SMD-FF study group. There was no correlation between the genotype and the L/M-cone–driven ERGs.

Conclusions. The changes in L/M-cone–driven ERG sensitivity and phase possibly represent two independent disease processes. The phase changes are similar to those found in patients with retinitis pigmentosa and possibly are a general feature of retinal dystrophies. (*Invest Ophthalmol Vis Sci.* 2001;42:1380–1389)

Stargardt's macular dystrophy (SMD) including fundus flavimaculatus (FF) is one of the most frequent causes of early macular degeneration and accounts for 7% of all retinal dystrophies.[1] It is an autosomal recessive condition characterized by a bilateral loss of central vision occurring early in life. Stargardt first described the disease as a unique macular dystrophy characterized by visual loss in the first two decades of life in combination with an atrophic lesion of the macula.[2] The term fundus flavimaculatus was first used by Franceschetti and denotes a retinal dystrophy characterized by yellow flecks found in the distal retina at the posterior pole of the eye.[3] Recently, it has been shown by linkage analysis that SMD and FF are the same disorder genetically.[4]

Mutations in the gene *ABCA4*, which encodes the photoreceptor-specific, adenosine triphosphate (ATP)-binding cassette transporter ABCA4, are responsible for SMD-FF.[5,6] Originally, it was found that *ABCA4* was expressed in rods, but not in cone photoreceptors,[5] which was surprising, because SMD-FF involves symptoms mostly related to cone dysfunction.[7,8] Recently, it was shown by immunofluorescence microscopy and Western blot analysis that ABCA4 is present in foveal and peripheral cones, as well as in rod photoreceptors, and that the cone-related dysfunctions are a direct consequence of ABCA4-mediated cone degeneration.[9] However, a morphologic differentiation between L- and M-cones was not possible.

We have developed a stimulus technique that allows the study of the long (L)- and middle (M)-wavelength–sensitive cone pathways and their interactions functionally by means of the electroretinogram (ERG).[10–12] This technique has been used to investigate the L- and M-cone (L/M-cone)–driven ERGs in patients with retinitis pigmentosa (RP), a retinal disorder in which the primary defect is located within the rod photoreceptors.[13] We found that the ERG sensitivity for both the L- and M-cone–driven ERGs was reduced and that there were large phase differences between the two. It is not evident what changes in the L/M-cone–driven ERGs occur when the cone system is thought to be primarily involved, as in SMD-FF. It was the purpose of the present study to investigate in detail L- and M-cone functions and their interactions in a large set of patients with SMD-FF and to correlate these findings with clinical features, genotype, and standard ERG techniques in a multidisciplinary approach.

Methods

Patients with SMD-FF and Normal Subjects

Forty-seven patients (age range, 13–59 years; mean, 32.9) participated in the study. A detailed history (including family history), visual acuity, visual fields (Tübingen automated perimeter; Oculus Optikgeräte, GmbH, Wetzlar, Germany), ganzfeld electroretinography according to the International Society for Clinical Electrophysiology of Vision (ISCEV) standard[14] (including the standard photopic 30-Hz-flicker ERG [30-Hz-fERG]), and multifocal electroretinography[15] were recorded and formed the basis for the diagnosis of SMD-FF. Color vision was screened in 43 patients by the Lanthony D-15 desaturated test.[16] This arrangement test allows a semiquantitative evaluation of color vision disorders. A discrimination between protan and deutan color vision deficiencies is virtually impossible, whereas a discrimination between tritan and protan-deutan deficiencies is easily achieved. We described

From the [1]Department of Experimental Ophthalmology, University Eye Hospital, Tübingen, Germany; the [2]Department of Medical Biometry, University of Tübingen, Germany; and the [3]Institute of Human Genetics, Biocenter, University of Würzburg, Germany.

Supported by Fortüne-Grant 707-0-0, Tübingen, Germany (HPNS, JK); Grant SFB 430/C3 from Deutsche Forschungsgemeinschaft (DFG), Heisenberg Fellowship Kr 1317/5-1, and Joint Grant 01 KS 9602, Project nr IB2, from the German Ministry for Education and Research and the University of Tübingen (JK); and DFG Grant 1259/10-1 (BHFW).

Submitted for publication July 6, 2000; revised November 14, 2000 and January 21, 2001; accepted January 31, 2001.

Commercial relationships policy: N.

The publication costs of this article were defrayed in part by page charge payment. This article must therefore be marked "*advertisement*" in accordance with 18 U.S.C. §1734 solely to indicate this fact.

Corresponding author: Jan Kremers, Department of Experimental Ophthalmology, University Eye Hospital, Röntgenweg 11, 72076 Tübingen, Germany. jan.kremers@uni-tuebingen.de

TABLE 1. Characteristics of the Patients with SMD-FF

Patient	Sex	Age (y)	Age at Onset (y)	VA	CFC	DF	CV	Exon (1)	Mut (1)	Exon (2)	Mut (2)
1	M	32	29	0.6	Moderate	+	Normal	48	L2241V		NF
2	F	39	23	0.4	Moderate	−	Chaotic	14	W663X	42	G1961E
3	M	34	16	0.1	Moderate	+	—	42	G1961E		NF
4	M	49	17	0.1	Severe	+	NP	6	G768T/splice	42	G1961E
5	F	36	35	0.6	Moderate	+	VS (T)	6	C230S	42	G1961E
6	M	28	17	0.1	Mild	++	INS	40	R1898H	43	G1975R
7	M	20	9	0.05	Moderate	++	VS (P/D)	12 + 21	L541P + A1038V	40	IVS40 + 5G → A
8	M	33	6	0.1	Mild	−	Chaotic		NF		NF
9	M	39	29	0.2	Moderate	+	VS (P/D)	13	G607R	42	G1961E
10	M	38	22	0.1	Severe	+	Chaotic		NF		NF
11	F	28	20	0.7	Mild	++	INS	3	A60T	40	R1898H
12	M	46	30	0.5	Mild	+	Chaotic	11	E471K	42	G1961E
13	F	25	11	0.1	Moderate	++	S	17	G863A		NF
14	F	51	41	0.8	Moderate	++	NP	40	R1898H		NF
15	F	23	17	0.1	Mild	−	Chaotic	3	P68L	36	S1689P
16	F	33	30	0.4	Mild	−	Chaotic	28	E1399K	42	G1961E
17	F	41	36	0.1	Severe	+	VS (T)	29	F1440V	37	G1748R
18	M	59	54	0.1	Severe	+	VS (P/D)	42	G1961E		NF
19*	M	35	15	0.05	Moderate	+	Chaotic	17	G863A	37	Q1750X
20*	M	43	14	HM	Severe	++	NP	17	G863A	37	Q1750X
21	F	46	16	0.1	Moderate	+	NP		NF		NF
22	F	32	22	0.05	Moderate	+	INS	21	A1038V		NF
23	M	50	42	0.3	Severe	++	VS (P/D)	12 + 21	L541P + A1038V	17	G863A
24	F	30	14	0.1	Moderate	++	INS	17	G863A	40	IVS40 + 5G → A
25	M	36	25	0.5	Moderate	++	—	3	296INSA	21	A1038V
26	M	40	23	0.2	Moderate	+	S	3	296INSA	42	G1961E
27	F	35	9	0.1	Severe	++	VS (P/D)	22	R1108C		NF
28	F	23	18	0.05	Mild	++	S	28	E1399K	43	G1977S
29	F	25	18	0.2	Mild	+	Chaotic	37	L1763P		NF
30	F	16	11	0.1	Moderate	+	Chaotic	22	R1108C		NF
31	M	40	35	0.1	Moderate	++	VS (P/D)	14	R681X		NF
32	F	28	27	0.1	Moderate	+	S	12 + 21	L541P + A1038V	21	A1038V
33	M	32	9	0.05	Severe	++	Chaotic	28	Q1412X	45	R2077W
34	F	23	21	0.2	Moderate	+	INS	6	G768T/splice		NF
35	F	38	33	FC	Moderate	−	Chaotic	17	G863A		NF
36	F	39	10	HM	Severe	++	NP		NF		NF
37	F	13	8	0.1	Moderate	++	S		—		—
38	F	27	25	0.2	Moderate	+	Chaotic	17	G863A	28	Q1412X
39	M	16	15	0.1	Moderate	+	VS (P/D)	12 + 17	R572Q + G863A	35	IVS35 + 2T → A
40	M	27	26	0.6	Moderate	−	S	17	G863A		NF
41	M	18	16	0.2	Moderate	+	—		—		—
42	M	25	24	0.1	Mild	−	—		NF		NF
43	F	29	9	0.1	Moderate	+	Chaotic	12 + 21	L541P + A1038V	42	G1961E
44	M	39	28	0.1	Mild	−	NP	6	N247S		NF
45	F	23	12	0.05	Mild	−	NP	6	R212C	19	T959I
46	M	43	36	0.2	Moderate	+	VS (P/D)	21	A1038V		NF
47	M	21	18	0.4	Mild	++	INS	28	Q1412X		NF

Shown are age at examination, age of onset, visual acuity, central fundus changes, and existence and distribution of the typical white-yellow flecks. In addition, the score from the Lanthony D-15 desaturated test (CV) and the molecular genetic findings in the *ABCA4* gene are specified (patients 37 and 41 were not screened for mutations in the *ABCA4* gene). VA, visual acuity; CFC, central fundus changes; DF, distribution of flecks; CV, color vision; FC, visual acuity dropped to finger counting; HM, visual acuity dropped to hand motions; CV test results: INS, insignificant; S, significant; VS, very significant; T, tritan; P/D, protan/deutan; NP, not possible; NF, not found.

* Patient 19 and 20 were siblings.

the results of this arrangement test by a categorization scheme from normal (no error), insignificant (one or more adjacent tablets confused), significant (two confusions between nonadjacent tablets), very significant (numerous confusions along one major axis: protan, deutan, or tritan), chaotic, and arrangements not feasible (because the patient was not able to discriminate any differences in color).[17]

Fundus appearances were assessed by slit lamp biomicroscopy and color fundus photographs. In the literature, there is no uniform classification of the fundus changes in SMD-FF. We staged the central fundus changes from mild (normal to diffuse foveal reflex, subtle pigment mottling of the macular retinal pigment epithelium [RPE], tapetal sheen or beaten-bronze reflex), moderate (pronounced hyper- and hypopigmentations of the macular RPE, bull's-eye pigment appearance, choroidal atrophic areas not larger than the typical fundus flecks) to severe (larger areas of choroidal atrophy). In addition, the existence and distribution of the typical white-yellow flecks at the level of the RPE and/or the choroidal atrophy were staged (scoring: −, no flecks and choroidal atrophy; +, flecks and choroidal atrophy confined to the posterior pole, i.e., within the vascular arcades; and ++, peripheral flecks and choroidal atrophy extending beyond the vascular arcades). Recently, the distribution of the fundus flecks has been similarly classified.[18] A summary of the findings in all 47 patients with SMD-FF is given in Table 1.

Twenty-nine normal subjects (age range, 9–57 years; mean, 29.2) served as a control. The age of the subjects in each population did not differ significantly (unpaired *t*-test). More detailed ERG data on a

subpopulation of the normal subjects have been published previously.[10] Informed consent was obtained from all subjects after explanation of the purpose and possible consequences of the study. The study was conducted in accordance with the tenets of the Declaration of Helsinki and with the approval of our institutional ethics committee on human experimentation.

ERG Recording

The method of ERG recording has been described before.[10,11] Briefly, the stimuli were presented on a computer-controlled monitor (Barco CCID 121; Vartech, Baton Rouge, LA) driven at 100 Hz by a graphics card (VSG 2/3; Cambridge Research Systems, Rochester, UK). The monitor subtended 124° by 108° at the 10-cm viewing distance. We used a 30-Hz square-wave modulation of the red, green, and blue phosphor with predefined Michelson contrasts. The time-averaged luminance of the monitor was 66 candelas (cd)/m^2 (40 cd/m^2 for the green phosphor, 20 cd/m^2 for the red phosphor, and 6 cd/m^2 for the blue phosphor). The time-averaged chromaticity in International Commission on Illumination (CIE; 1964) large-field coordinates was: $x = 0.3329$, $y = 0.3181$. The excitation in each cone type by the monitor phosphors was calculated by multiplying the phosphor emission spectra with the psychophysically based fundamentals.[19]

The modulation of cone excitation was quantified by the Michelson cone contrast and defined the stimulus strength for each cone type separately. The short (S)-wavelength cones were silently substituted in all conditions (S-cone contrast was 0%). In 10 of the 47 patients with SMD-FF and 19 of the 29 normal subjects, we measured ERG responses to 32 different stimuli: eight conditions of different L-/M-cone contrast ratios (1:1, −1:1, 1:2, 0:1, 2:1, −2:1, −1:2, and 1:0) with four contrasts at each condition (100%, 75%, 50%, and 25% of the maximally possible cone contrast). An L-/M-cone contrast ratio of 1:1 corresponds to an in-phase modulation of the L/M cones with equal cone contrast; an L-/M-cone contrast ratio of −1:1 corresponds to a modulation of the two cone types in counterphase with equal cone contrast; an L-/M-cone contrast ratio of 1:2 corresponds to an in-phase modulation of the two cone types with the M-cone contrast twice as much as the L-cone contrast; and an L-/M-cone contrast ratio of 0:1 corresponds to a silent substitution of the L cones. In 35 of the 47 patients with SMD-FF and in 10 of the 29 normal subjects, we limited the measurements to the four most important conditions with L-/M-cone contrast ratios of 1:1, 1:0, 0:1, and −1:1, which allowed us to obtain reliable amplitude data and, simultaneously, direct measurements of response phases to cone-isolating stimuli. In patient 7, five conditions were used; in patient 5, only ERG measurements to the cone-isolating conditions were performed.

ERG recordings were obtained from one eye in all subjects. Because SMD-FF usually affects both eyes rather homogeneously, one eye was randomly chosen (in both subject groups). The pupils of the control subjects' eyes were dilated with 0.5% tropicamide, and those of the patients' eyes with both 0.5% tropicamide and 5% phenylephrine. The pupil diameter was recorded before each experiment. There was no significant difference in pupil diameter between the two subject groups. The eyes were kept light-adapted for at least 10 minutes before the ERG recording.

Corneal ERG responses were measured with DTL fiber electrodes that were positioned on the conjunctiva directly beneath the cornea and attached with their two ends at the lateral and nasal canthus. The reference and skin electrodes (gold cup electrodes) were attached to the ipsilateral temple and the forehead, respectively. The signals were amplified and filtered between 1 and 300 Hz (Grass, Quincy, MA) and sampled at 1000 Hz with a data acquisition card (AT-MIO-16DE-10; National Instruments, Austin, TX). ERG responses to 12 runs, each lasting 4 seconds, were averaged in each measurement. The ERG response amplitudes and phases were extracted from a discrete Fourier transform (DFT) of the responses and were defined as the amplitudes and phases of the fundamental component.

Mutation Analysis in the *ABCA4* Gene

Forty-five of the 47 patients who participated in the study were screened for alterations in the *ABCA4* gene. DNA was extracted from peripheral blood according to standard protocols. All 50 exons of the *ABCA4* gene were analyzed by a combination of denaturing gradient gel electrophoresis (DGGE), denaturing high-performance liquid chromatography (DHPLC), and single-strand conformation polymorphism (SSCP) analysis as described in detail elsewhere.[6] Briefly, each exon was subjected to polymerase chain reaction (PCR) amplification with oligonucleotide primers designed to amplify the coding region and splice junctions. For DGGE, the PCR products were electrophoresed on a 6% polyacrylamide gel containing a 20% to 70% (exons 1, 3, 4, 6, 7, 9, 12–16, 18–26, 28, 29, 31, 33, 25–37, 39–43, 45–48, and 50) or 0% to 70% (exons 2, 5, 17, 32, and 34) gradient of urea and formamide. To optimize the sensitivity in mutation detection, the PCR products corresponding to exons 8, 27, 30, 38, 44, and 49 were also subjected to DHPLC.[20] For SSCP (exons 10 and 11), the PCR-amplified fragments were analyzed on a 6% nondenaturing polyacrylamide gel with 5% glycerol at 4°C. For each technique used, all aberrant fragments were directly DNA sequenced by using a kit (PRISM Ready Reaction Sequencing Kit; Perkin Elmer–Cetus, Norwalk, CT) and an automated sequencer (AB310; Perkin Elmer–Applied Biosystems, Foster City, CA).

Results

ERG Responses and Model Fits

In Figure 1 original ERG tracings of a patient with SMD-FF (thick line) and a normal subject (thin line) are shown to a standard 30-Hz-flicker (ganzfeld; Fig. 1A), to pure L-cone modulation (Fig. 1B), and to pure M-cone modulation (Fig. 1C). Patient 25 exhibited mild clinical changes, and the genetic analysis revealed a 296insA mutation in exon 3 and an A1038V mutation in exon 21 (Table 1). His ganzfeld white 30-Hz-fERG signal was reduced in amplitude and somewhat advanced (Fig. 1A). His L-cone–driven ERG signal displayed only minimal differences in comparison with the normal subject (Fig. 1B), whereas his M-cone–driven ERG signal was considerably phase advanced and lower in amplitude (Fig. 1C).

In Figure 2, the mean response amplitudes of normal subjects and patients in the L/M-cone–isolating conditions are displayed as a function of cone contrast. The relationship between ERG response amplitude and cone contrast was close to linear in all conditions and in both the patients with SMD-FF and the normal subjects (Fig. 2).

The slope of the linear regression of the data is the increase in ERG amplitude per percentage increase in cone contrast. This slope was used to define the cone contrast gain. The inverse of the cone contrast gain is the increase in cone contrast needed for a 1-μV response increase,[10] which, owing to the linear relationship between amplitude and cone contrast, is equivalent to a threshold. The cone contrast gains and the thresholds were obtained for all ratios of L-/M-cone contrasts.

Figure 3A shows the measured ERG thresholds for three normal subjects. The ellipses are fits of a model, based on the assumption that the signals originating in the L- and M-cones are vector summed in the total ERG response. A detailed description of the model can be found elsewhere.[10] Briefly, we assume that the signals originating in the L/M cones have separate weightings (defined by the cone contrast gains) and phases and that the total response is simply the addition of the two separate responses at each instant. Because the responses are basically sinusoidal in shape without intrusion of higher harmonics (see also Reference 12), they can be expressed as vectors, the lengths of which are determined by the amplitudes. The angles formed with the positive *x*-axis are equiva-

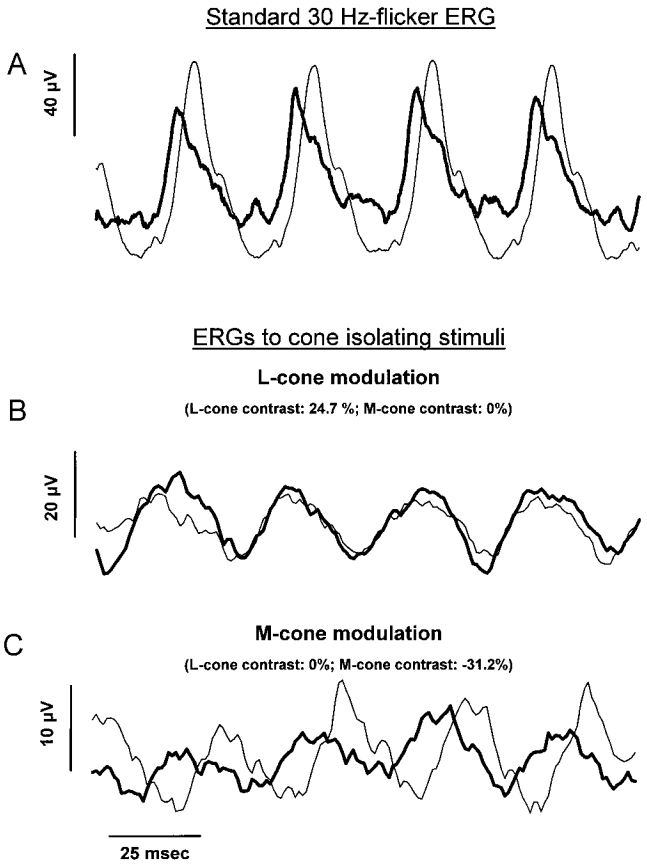

FIGURE 1. Averaged standard 30-Hz-fERG responses (ganzfeld; **A**) and ERG responses to pure L-cone (**B**) and M-cone modulation (**C**) in a patient with SMD-FF (*thick line*) and a normal subject (*thin line*). The ERG signals are 150-msec extracts. The L/M-cone–driven ERGs were approximately in counterphase in the normal subject, mainly caused by the counterphase stimulation of the L- and M-cones. The L/M-cone tracings are from the same time windows of the recordings, enabling a mutual comparison. Drift in the ERG responses to the L/M-cone–isolating stimuli were suppressed by removing low-frequency components. Patient 25, who had a mild phenotype carrying a 296insA mutation in exon 3 and an A1038V mutation in exon 21, exhibited reduced standard 30-Hz-fERG signals that were somewhat advanced compared with the normal subject (**A**). His L-cone–driven ERG signal was even larger and somewhat delayed compared with that of the normal subject in (**B**), whereas his M-cone driven ERG signal was considerably phase advanced and lower in amplitude (**C**).

lent to the phases. According to this assumption, the response vector to a combination of L/M-cone modulation is equal to the addition of the two vectors derived from the responses driven by each cone. In the fits of this model to the threshold data, there are three free parameters: the L-cone weighting or L-cone contrast gain (A_L), the M-cone weighting or the M-cone contrast gain (A_M), and the phase difference between the L- and M-cone–driven responses ($|P_L - P_M|$).

As has been reported previously in normal subjects[10] and in patients with RP,[13] there is a considerable interindividual variability of the L-/M-cone weighting ratio reflected by the different orientations of the ellipses. The larger the L-/M-cone weighting ratio, the more the thresholds' ellipses are tilted toward the M-cone axis. This variability can be correlated with variations in the L-/M-cone weighting ratios in psychophysical tasks that tap the luminance channel and probably can be attributed to the variability in the number of L and M cones in the human retina.[21,22] Despite the variability, the major axes of the ellipses of all normal subjects are located within the second and fourth quadrants, indicating additive interactions between the signal originating in the L and M cones and that the phase difference $|P_L - P_M|$is always smaller than 90° in the normal subjects.

Figure 3B shows the ERG thresholds for nine patients with SMD-FF. There is also a considerable interindividual variability of the L-/M-cone contrast gain ratio. However, we encountered patients who displayed additive interactions between the L/M-cone–driven ERGs (Fig. 3B, upper row), but also patients for whom the cone-driven signals were more or less independent (Fig. 3B, middle row) or subtractive (Fig. 3B, lower row). As a result, the phase differences could be smaller than 90° (additive interactions), approximately orthogonal (independent actions), or larger than 90° (subtractive interactions). Thus, the variability in phase difference was considerably larger than in the normal subjects.

Cone Weightings and ERG Sensitivity

The L-/M-cone weightings (A_L and A_M, respectively) estimated from the model fits to the threshold data were statistically analyzed with an analysis of variance (ANOVA). The ANOVA revealed that the cone weightings differed significantly in the groups defined by subject group and cone type ($P < 0.0001$; $F = 36.46$). Post hoc tests for subsequent multiple comparisons between subject groups and cone type, using Tukey–Kramer's honestly significant difference (HSD; $\alpha = 0.05$), revealed that the average A_L of the normal subjects (0.293) was significantly larger than the average A_M (0.112). Similarly, in the patients A_L (0.292) was significantly larger than A_M (0.088). However, A_L and A_M did not differ between the subject groups (Fig. 4A).

From the cone weightings we calculated the individual L-/M-cone weighting ratios (Fig. 4B). These ratios do not have

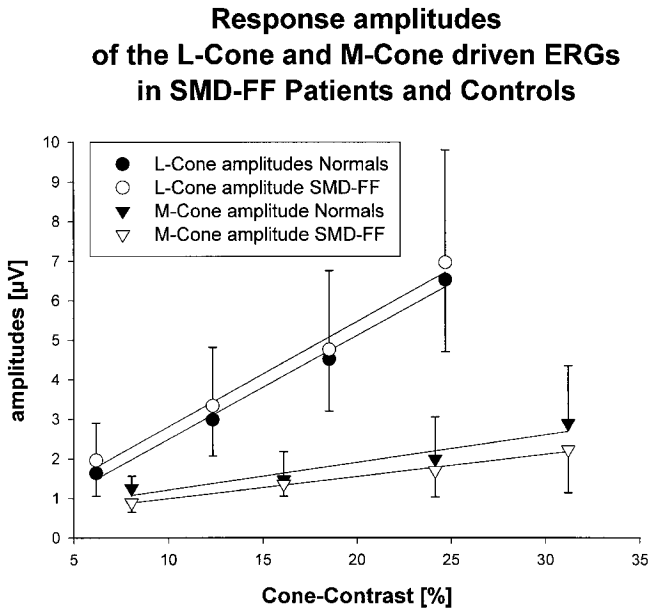

FIGURE 2. ERG response amplitude to cone-isolating stimuli as a function of cone contrast in normal subjects and patients with SMD-FF (mean ± SD). The data show that there is a linear relationship between ERG response amplitude and cone contrast. The slopes of the linear regressions are equivalent to the cone contrast gain. The linear regressions of the L-cone–driven ERG could be described by $f(x) = -0.1 + 0.26 \cdot x$ for the control group and $f(x) = 0.1 + 0.27 \cdot x$ for the SMD-FF group. The linear regressions of the M-cone–driven ERG could be described by $f(x) = 0.5 + 0.07 \cdot x$ for the control group and $f(x) = 0.4 + 0.06 \cdot x$ for the SMD-FF group.

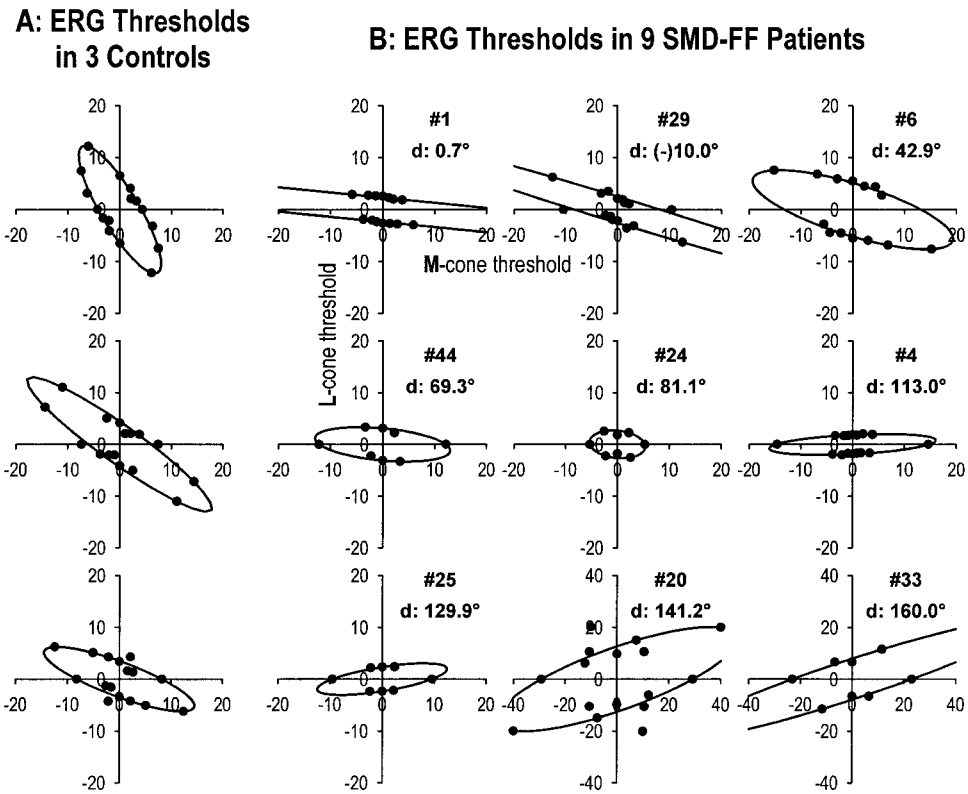

FIGURE 3. Threshold contrasts in three normal subjects (**A**, *left*) and nine patients with SMD-FF (**B**, *right*). The ellipses are fits of a vector-addition model to the data points.[10] There was a substantial interindividual variability for the phase difference between L/M-cone–driven ERG responses in the patient group. In a subset of the patients with SMD-FF (*lower three panels*), the major axis of the displayed ellipses is tilted towards the first and third quadrant, indicating phase differences that are larger than 90°, resulting in a subtractive interaction between the signals originating in the L-cones and the M-cones. The mean maximal sensitivity (quantified by the smallest possible distance of the fitted ellipse to the origin) was more variable in the patients with SMD-FF (indicated by the different scaling used for two patients with SMD-FF).

a normal distribution, making a standard test difficult. We therefore converted the ratios into their logarithms that are normally distributed. An unpaired *t*-test on these data did not reveal a significant difference between the ratios in the patients with SMD-FF and the control subjects.

Because of the large interindividual variability of L-/M-cone weightings, neither of them can be directly used to quantify the overall ERG sensitivity of individual patients. We therefore quantified the mean maximal sensitivity (S_m) by determining the theoretically least threshold defined as the smallest possible distance of the fitted ellipse to the origin. This smallest possible distance can be estimated analytically from the model fits.[13] Bartlett's F-test revealed that the variability of S_m in the SMD-FF group was significantly larger than in the control group ($P = 0.01$; $F = 6.12$). A subsequent Welch's *t*-test (allowing a comparison between groups with unequal SDs) revealed that, on average, the S_m of the patients with SMD-FF (0.301 ± 0.113 $\mu V \cdot [\%\ \text{cone contrast}]^{-1}$) did not differ significantly ($P = 0.4$) from that of the normal subjects (0.320 ± 0.072 $\mu V \cdot [\%\ \text{cone contrast}]^{-1}$; Fig. 4C).

To test for the relationship between S_m and other clinical parameters (disease duration, visual acuity, central fundus changes, distribution of flecks; Table 1), we used an analysis of covariance (ANCOVA). To partial out the obvious dependency of disease duration on age, we corrected disease duration for age. In the ANCOVA, we tested a model in which it was assumed that the variability in S_m can be explained by four factors: age-adjusted disease duration, visual acuity, central fundus changes, and distribution of flecks. Model fit was unsatisfactory (adjusted $R^2 = 0.14$; root mean square error = 0.10 $\mu V \cdot [\%\ \text{cone contrast}]^{-1}$). Neither the age-adjusted disease duration nor the other factors were significantly related to S_m.

Phases of Cone-Driven ERGs

The phases of the L/M-cone–driven ERGs were obtained directly from the Fourier analysis of the ERG responses to the cone-isolating stimuli. In Figure 5, the ERG response phases for the M- and L-cone–isolating stimuli are shown as a function of cone contrast (provided that the response amplitudes were significantly above noise level, typically being approximately 0.3 μV). As has been observed previously for normal subjects,[12,23] the ERG response phase lag decreased linearly with increasing cone contrast for both subject groups within the range of used cone contrasts (but see Reference 12 for the case when low cone contrasts are included).

We applied an ANCOVA to these phase data to correct for the influence of cone contrast. We assumed that the variability in the data could be explained by four factors: subject group (normal subjects, patients with SMD-FF), cone type, cone contrast, and subject number as a random effect. Further, it was assumed that these factors could interact, that all measurement errors were identical, and that there was a linear relationship between response phase and cone contrast. As a result, four different straight lines were estimated describing the relationship between response phase and cone contrast for each subject group and each cone type by the ANCOVA (Fig. 5). Model fit was good (adjusted $R^2 = 0.67$; root mean square error = 26.1°). Subject groups differed significantly ($P = 0.0038$), and there was a significant interindividual variability ($P < 0.0001$). There were interactions between cone contrast and subject group ($P < 0.0001$) and between cone contrast and cone type ($P < 0.0001$). Nested groups defined by subject group and cone type differed significantly ($P < 0.0001$).

The L-cone–driven ERG response phase lags decreased significantly with increasing cone contrast with a slope of 1.62 ± 0.36; $P < 0.0001$ in the normal subjects and a slope of 1.33 ± 0.29; $P < 0.0001$ in the patients with SMD-FF. The M-cone–driven ERG response phase lags also decreased with increasing cone contrast with a slope (±SE) of 1.16 ± 0.45 ($P = 0.01$) in the normal subjects and a slope of 0.50 ± 0.40 in the patients with SMD-FF, which was not significantly different from zero.

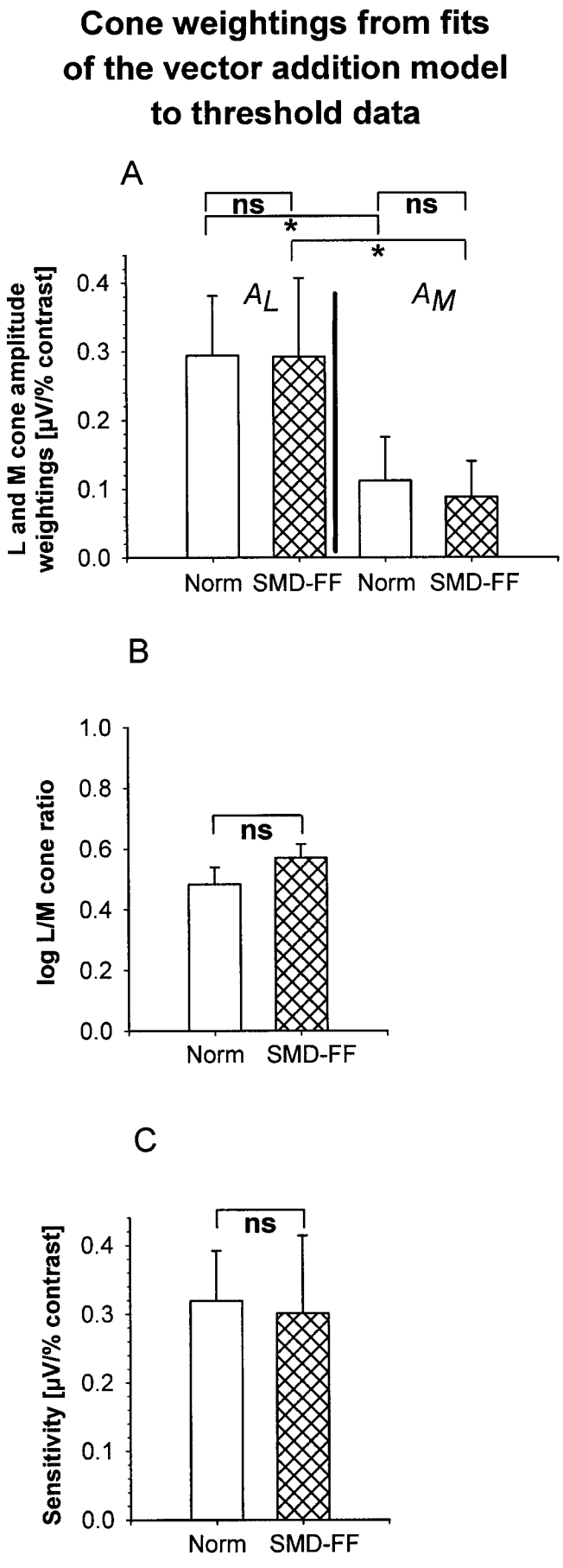

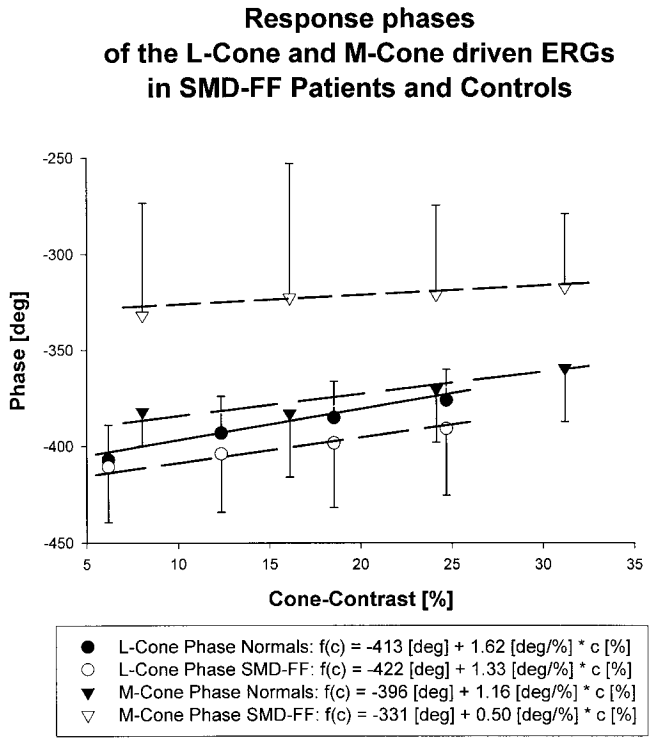

FIGURE 5. ERG response phase to cone-isolating stimuli as a function of cone contrast for the normal subjects and the patients with SMD-FF (mean ± SD). The response phases of the L-cone–driven ERGs were delayed, whereas the phases of the M-cone–driven ERGs were advanced in the patients with SMD-FF compared with the normal subjects. Four different straight lines describing the relationship between response phase and cone contrast for each subject group and each cone type were estimated with an ANCOVA.

From the ANCOVA, the mean ERG response phase, P_L and P_M (at 17.5% cone contrast), was estimated for each combination of subject group and cone type. Post hoc tests (Tukey–Kramer HSD; $\alpha = 0.05$) revealed that P_L of the patients with SMD-FF (−399°) lagged P_L of the control subjects (−385°) significantly and that P_M of the patients (−323°) was significantly phase advanced compared with the control group (−376°). P_L and P_M differed significantly in the patients with SMD-FF but not in the normal subjects (Fig. 6A). As a cause of the differential effect of SMD-FF on P_L and P_M, the mean phase difference of 76° (corresponding to 7.0 msec, when assuming that a difference in time delay is causing the phase difference) was considerably larger than the one in the normal subjects (9°; corresponding to an 0.8-msec delay difference). Independent estimates of the phase differences between L/M-cone–driven ERGs ($|P_L - P_M|$) were available from the model fits to

FIGURE 4. (**A**) Estimated L-/M-cone weightings (A_L and A_M: means ± SD) for the normal subjects and the patients with SMD-FF derived from the fits of a vector-addition model to the threshold data. The results of the ANOVA (post hoc tests) on the weighting data are displayed above the histograms (*, significant difference; ns, nonsignificant effect). (**B**) The L-/M-cone weighting ratio given as $\log(A_L/A_M)$ with mean ± SE. There was no significant difference between the normal subjects and the patients with SMD-FF. (**C**) The maximal L/M-cone–driven ERG sensitivity for the normal subjects and the patients with SMD-FF (mean ± SD). The SD in the SMD-FF group was significantly larger than in the group of normal subjects (Bartlett's F-test; $P = 0.01$). Welch's *t*-test did not reveal a difference between the mean maximal sensitivities of the SMD-FF group and the control group.

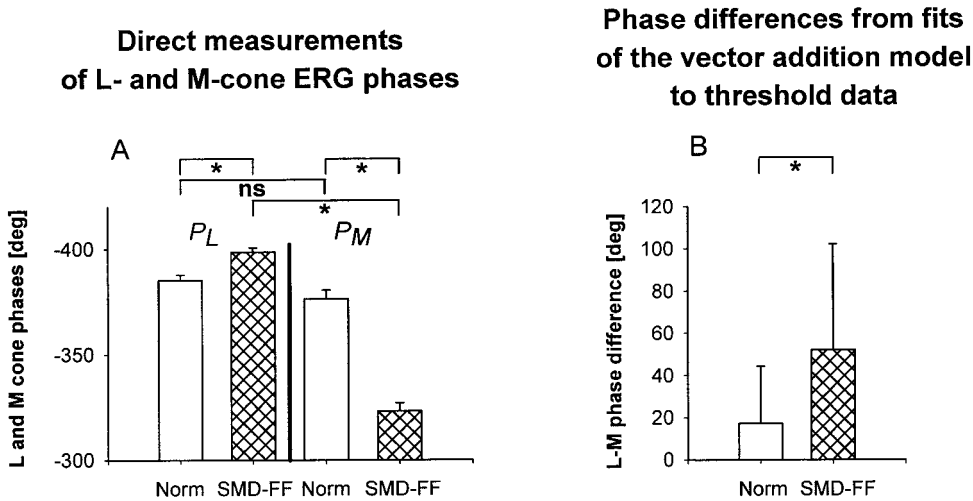

FIGURE 6. (**A**) Phase data for the normal subjects and the patients with SMD-FF derived directly from the ERG measurements with the cone-isolating stimuli (means ± SE). After correction for the effect of cone contrast, the phase lag of the L-cone–driven ERG response of the patients with SMD-FF was significantly increased, whereas the M-cone–driven ERG phase lag was significantly decreased. The results of the ANCOVA (post hoc tests) are indicated above the histograms (*, significant difference; ns, nonsignificant effect). (**B**) Phase differences between L/M-cone–driven ERGs estimated from the fits of a vector-addition model to the threshold data (means ± SD). The fit data revealed a highly significant increase in phase difference ($P = 0.001$; unpaired *t*-test). This increase is in accordance with the changes in ERG response phases obtained from the direct measurements.

the threshold data and displayed in Figure 6B. $|P_L - P_M|$ differed significantly between patients and control subjects ($P = 0.001$; unpaired *t*-test).

Both measures correlated closely in both the control group ($r = 0.82$) and the SMD-FF group ($r = 0.86$; Fig. 7). For the combined groups, the correlation coefficient was 0.87 (95% confidence interval, 0.77–0.92).

To test for the relationship between the clinical parameters (age-adjusted disease duration, visual acuity, central fundus changes, and distribution of flecks; Table 1) and $|P_L - P_M|$, an ANCOVA was used. Model fit was satisfactory (adjusted $R^2 = 0.39$; root mean square error = 38.8°). However, only age-adjusted disease was significantly correlated with $|P_L - P_M|$ ($P = 0.04$).

Comparison of the L/M-Cone–Driven ERGs and Color Vision Test

The majority of the patients with SMD-FF exhibited pronounced color vision disturbances (Table 1). Ten patients showed significant color vision disturbances with confusions along a major axis. However, there was no obvious correlation of the extent or the type of color vision with any of the values derived from the L/M-cone–driven ERG measurements. None of the patients had ERGs that were exclusively determined by either L- or M-cone activity, as is described for patients with dichromatism who have inherited red-green color vision defects.[10]

Comparison of the L/M-Cone–Driven ERGs and the Standard 30-Hz fERG

S_m, $|P_L - P_M|$ were correlated with the amplitude and implicit times of the 30-Hz fERG. The Bonferroni–Holm test was performed to correct for multiple comparisons (multiple $\alpha = 0.05$). S_m correlated positively with the amplitude ($r = 0.67$) and negatively with the implicit time ($r = -0.38$) of the 30-Hz fERG. In addition, $|P_L - P_M|$ correlated negatively with the amplitude ($r = -0.39$) and positively with the implicit time ($r = 0.53$) of the 30-Hz fERG. There was no significant correlation between the logarithm of the L-/M-cone weighting ratio and the two parameters of the 30-Hz fERG.

Mutation Analysis in the *ABCA4* Gene

ABCA4 alterations were detected in 40 of the 45 patients studied (Table 1). Two disease alleles were identified in 24 subjects including two affected brothers, whereas only a single mutant allele was detectable in 16 patients (Table 1). Fifty missense mutations made up the majority of the 64 *ABCA4* alterations detected. In addition, seven nonsense mutations were identified (five mutations affecting RNA splicing; two single–base-pair insertions causing a frameshift), all of which are considered to be moderate or severe alleles, because they are expected to result in a truncated protein. Homozygosity for a moderate or severe allele was not observed.

The numbers of occurrence of each present mutation were too small to make any specific correlation between mutation and clinical phenotype. In general, however, no obvious relationships were evident between the type of identified mutation or its position within the gene and S_m or with $|P_L - P_M|$. Similarly, no correlation was apparent between mutation type and position with the presence and distribution of flecks or the severity of fundus changes.

DISCUSSION

Correlation with Clinical Features

There is some controversy about whether there is a correlation between funduscopically visible fundus changes and functional abnormalities in SMD-FF. Classification of the fundus changes has been controversial.[24–27] We classified the patients by two funduscopic criteria: the distribution of flecks (similar to the classification of Hadden and Gass[18]) and the severity of the central fundus changes. None of these measures, however, correlated with the amplitude and phase features of the L/M-cone–driven ERGs, which is in accordance with the findings of

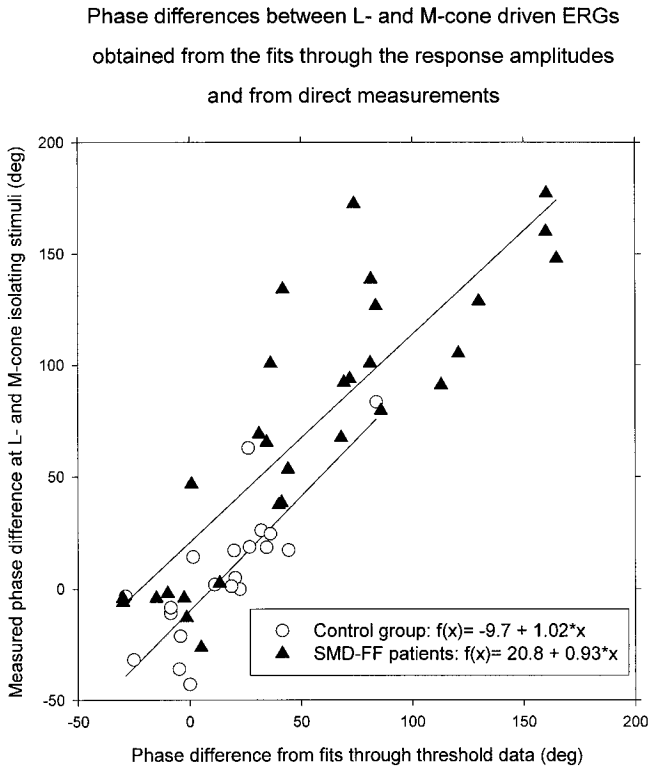

FIGURE 7. Phase differences between L/M-cone–driven ERG responses obtained from the direct measurements as a function of the phase differences obtained from the model fits to the threshold data for individual normal subjects and patients with SMD-FF. For the direct measurements, ERG response phases at 24.7% L-cone contrast and 23.4% M-cone contrast data were considered. (Response phases at similar cone contrasts were used to minimize contamination by the influence of cone contrast.) The fits provided only absolute values of phase differences and therefore are not conclusive about which cone response was leading. The authors decided to give the phase differences calculated from the model fits the same sign as those obtained from the direct measurements: Positive-phase differences indicate that the M-cone–driven ERG responses were leading; negative-phase differences indicate that the L-cone–driven ERG responses were leading (see also Fig. 6 in Kremers et al.[10]). The description of the linear regression describing the relationship between the two values is given in the legends. For both the patients with SMD-FF ($r = 0.86$; $P < 0.0001$) and the normal subjects ($r = 0.82$; $P < 0.0001$), the two regressions had very similar slopes, but larger phase differences were observed in a subset of the patients with SMD-FF.

several studies using standard ERG techniques,[24,28,29] but contradicts others.[25,30–32]

Another matter of debate is whether functional abnormalities are correlated with the disease duration. Noble and Carr[24] did not find such a correlation. In contrast, Armstrong et al.[32] found a significant correlation of ERG amplitudes and implicit times with age-adjusted disease duration for the FF group but not for the SMD group, whereas Moloney et al.[28] found the opposite. We found $|P_L - P_M|$ to be significantly correlated with duration, but not the overall ERG sensitivity S_m. This may suggest that $|P_L - P_M|$ and S_m represent two independent disease processes. Only $|P_L - P_M|$ appears to be a useful measure for evaluating the disease and monitoring its progression.

The fact that there was no correlation between the color vision disturbances and the ERG data is not surprising, because color vision tasks such as the Lanthony D-15 desaturated test represent psychophysical measurements exclusively testing the macula. The data of our ERG measurements, however, reflect the function of a much larger part of the retina. Furthermore, we recently established that the processing of cone signals in the chromatic channel and in the ERG is mutually independent.[21] A change in the ERG is probably also independent of changes in the chromatic channel.

Correlation with Genotype

It has been proposed that residual ABCA4 protein activity determines the clinical phenotype of SMD-FF and other related retinal diseases, whereas the pairing of two null or severe mutations is thought to lead to a more severe phenotype resembling a cone–rod dystrophy or inverse RP.[33–35] The mutation profile in our group of patients with SMD-FF (with two identified mutations) is in concordance with this model, because only a combination of a mild and severe mutation (e.g., G1961E and 296insA) or of two moderate mutations (e.g., IVS40+5G→A and A1038V) were encountered, whereas the pairing of two null or severe mutations was not observed in our patient sample. Within the patient group, however, no phenotypic distinctions associated with genotype were apparent. We did not find an association between mutation type and the presence of flecks or severity of fundus changes, nor did we note any association with the functional alterations.

Correlation with Standard ERG Techniques

Several groups have investigated the amplitudes and implicit times of the photopic standard ERG in SMD-FF with differing results.[18,24–32,36] Recently, we argued that the 30-Hz fERG can be misinterpreted, because its amplitude depends not only on overall ERG sensitivity (S_m) but also on the phase difference between the L/M-cone–driven ERG ($|P_L - P_M|$).[13] This hypothesis is now statistically validated in the large group of patients with SMD-FF. Moreover, because the phase changes are different for the L/M-cone–driven ERGs, the amplitudes rather than the implicit times of the 30-Hz fERG reveal the actual timing changes within the individual cone pathways. Thus, the 30-Hz fERG is a signal that depends in a complex manner on its constituent components and is therefore difficult to interpret.

Origins of Selective Changes of L/M-Cone–Driven ERGs

It has been found that in SMD-FF the *ABCA4* gene is defective, resulting in a change in the rod ABCA4 (rim protein), which is involved in the regeneration of rhodopsin.[37,38] These findings are in accordance with the observation that patients with SMD-FF show rod deficits.[25,39,40] In addition, Molday et al.[9] showed that ABCA4 is present in both cone and rod photoreceptors, suggesting that it is involved in the photopigment regeneration of both photoreceptor types.

It remains speculative to link these molecular findings with the functional alterations of the L/M-cone–driven ERG pathways. The change in the cone ERGs are possibly caused by either a change within the cones themselves, due to the defective ABCA4, or are the indirect result of an alteration within the RPE. However, it is difficult to conceive how any of these changes might lead to selective modification in the L/M-cone–driven ERG.

Recently, we found similar timing changes in patients with RP.[13] The phase difference between L/M-cone–driven ERGs was substantially increased. Some patients with SMD-FF (e.g., patients 17 and 87 in Fig. 3) showed similar phase differences. Because RP primarily affects the rod system, and the cone system is only secondarily affected, similar secondary cone alterations after primary rod modifications in SMD-FF cannot be excluded.

It is well established that the ERG at 30 Hz is the result of postreceptoral mechanisms, most probably at the bipolar cell level, involving both ON- and OFF-responses.[41] A selective

change in the ON- and OFF-components of the L/M-cone–driven ERGs may also lead to the described pattern in the patients with SMD-FF. However, on the basis of our data it is impossible to draw a definite conclusion on the responsible pathologic mechanism.

Are Temporal Alterations of L/M-Cone–Driven ERG Pathways a General Feature of Retinal Dystrophies?

Recently, we found large phase differences between the L/M-cone–driven ERGs in patients with RP[13] and to a lesser extent in patients with Best's macular dystrophy (BMD).[42] In the present report, we describe similar alterations in a large group of genetically screened patients with SMD-FF suggesting that such different alterations of the L/M-cone pathways indeed are a general feature of retinal dystrophies.

However, there are substantial differences between patients with RP and those with SMD-FF when both the amplitude and the timing data are taken into consideration. Furthermore, the dependency of the response phases on cone contrast seems to be different between different patient groups. The mean M-cone–driven ERG response phase P_M was significantly phase advanced in patients with SMD-FF (−323°), patients with RP[13] (−326°), and patients with BMD[42] (−345°) when compared with normal subjects (−376°). The mean L-cone driven ERG phase P_L was significantly phase delayed in patients with SMD-FF (−399°) and in patients with RP[13] (−486°), whereas P_L of the patients with BMD did not show a significant difference from that of normal subjects[42] (−383° and −385°, respectively). The mean L/M-cone–driven ERG sensitivity S_m, however, was normal in the patients with SMD-FF as a group (0.301 μV · [% cone contrast]$^{-1}$) compared with that in normal subjects (0.320 μV · [% cone contrast]$^{-1}$), whereas S_m was significantly decreased in patients with RP[13] (0.151 μV · [% cone contrast]$^{-1}$) and significantly increased in those with BMD[42] (0.493 μV· [% cone contrast]$^{-1}$). Furthermore, in normal subjects,[10,12] patients with BMD,[42] and patients with SMD-FF, both the L- and the M-cone–driven ERG phases are positively correlated with cone contrast, whereas in most patients with RP, there is a negative correlation.[13] We conclude that L/M-cone–driven ERGs can serve as a tool for a differential diagnosis of hereditary retinal disorders when both amplitude and phase criteria are considered.

Acknowledgments

The authors thank Eckart Apfelstedt–Sylla and Dorothea Besch for their clinical contributions; Kathrin Vohrer for technical assistance; and Eberhart Zrenner for general support.

References

1. Kaplan J, Gerber S, Larget PD, et al. A gene for Stargardt's disease (fundus flavimaculatus) maps to the short arm of chromosome 1. *Nat Genet.* 1993;5:308–311.
2. Stargardt K. Über familiäre, progressive Degenerationen im Kindesalter. *Graefes Arch Clin Exp Ophthalmol.* 1909;71:534–550.
3. Franceschetti A. Über tapeto-retinale Degenerationen im Kindesalter. In: Sautter H, ed. *Entwicklung und Fortschritt in der Augenheilkunde.* Stuttgart: Enke; 1963:107–120.
4. Anderson KL, Baird L, Lewis RA, et al. A YAC contig encompassing the recessive Stargardt disease gene (STGD) on chromosome 1p. *Am J Hum Genet.* 1995;57:1351–1363.
5. Allikmets R, Singh N, Sun H, et al. A photoreceptor cell-specific ATP-binding transporter gene (ABCR) is mutated in recessive Stargardt macular dystrophy. *Nat Genet.* 1997;15:236–246.
6. Rivera A, White K, Stohr H, et al. A comprehensive survey of sequence variation in the ABCA4 (ABCR) gene in Stargardt disease and age-related macular degeneration. *Am J Hum Genet.* 2000;67:800–813.
7. Sun H, Nathans J. Stargardt's ABCR is localized to the disc membrane of retinal rod outer segments. *Nat Genet.* 1997;17:15–16.
8. Illing M, Molday LL, Molday RS. The 220-kDa rim protein of retinal rod outer segments is a member of the ABC transporter superfamily. *J Biol Chem.* 1997;272:10303–10310.
9. Molday LL, Rabin AR, Molday RS. ABCR expression in foveal cone photoreceptors and its role in Stargardt macular dystrophy. *Nat Genet.* 2000;25:257–258.
10. Kremers J, Usui T, Scholl HPN, Sharpe LT. Cone signal contributions to electroretinograms in dichromats and trichromats. *Invest Ophthalmol Vis Sci.* 1999;40:920–930.
11. Usui T, Kremers J, Sharpe LT, Zrenner E. Flicker cone electroretinogram in dichromats and trichromats. *Vision Res.* 1998;38:3391–3396.
12. Usui T, Kremers J, Sharpe LT, Zrenner E. Response phase of the flicker electroretinogram (ERG) is influenced by cone excitation strength. *Vision Res.* 1998;38:3247–3251.
13. Scholl HPN, Kremers J. Large phase differences between L-cone and M-cone driven electroretinograms in retinitis pigmentosa. *Invest Ophthalmol Vis Sci.* 2000;41:3225–3233.
14. Marmor MF, Zrenner E. Standard for clinical electroretinography (update). *Doc Ophthalmol.* 1995;1994:89:199–210.
15. Kretschmann U, Seeliger MW, Ruether K, et al. Multifocal electroretinography in patients with Stargardt's macular dystrophy. *Br J Ophthalmol.* 1998;82:267–275.
16. Lanthony P, Dubois PA. Le Farnsworth 15 désaturé. *Bull Soc Ophtalmol Fr.* 1973;73:861–866.
17. Nimsgern C, Krastel H, Auffarth GU, Eggers I, Lang H. Standardisierte Prüfung des Rot-, Grün- und Blausinns: vergleich zwischen Farbfleck- und computergestütztem Testverfahren. *Ophthalmologe.* 1998;95:559–563.
18. Hadden OB, Gass JD. Fundus flavimaculatus and Stargardt's disease. *Am J Ophthalmol.* 1976;82:527–539.
19. Stockman A, MacLeod DIA, Johnson NE. Spectral sensitivities of the human cones. *J Opt Soc Am A.* 1993;10:2491–2521.
20. Liu W, Smith DI, Rechtzigel KJ, Thibodeau SN, James CD. Denaturing high performance liquid chromatography (DHPLC) used in the detection of germline and somatic mutations. *Nucleic Acids Res.* 1998;26:1396–1400.
21. Kremers J, Scholl HPN, Knau H, et al. L- and M-cone ratios in human trichromats assessed by psychophysics, electroretinography and retinal densitometry. *J Opt Soc Am A.* 2000;17:517–526.
22. Williams DR, Roorda A. The trichromatic cone mosaic in the human eye. In: Gegenfurtner KR, Sharpe LT, eds. *Color Vision: From Genes to Perception.* Cambridge, UK: Cambridge University Press; 1999:113–122.
23. Wu S, Burns SA, Elsner AE. Effects of flicker adaptation and temporal gain control on the flicker ERG. *Vision Res.* 1995;35:2943–2953.
24. Noble KG, Carr RE. Stargardt's disease and fundus flavimaculatus. *Arch Ophthalmol.* 1979;97:1281–1285.
25. Itabashi R, Katsumi O, Mehta MC, et al. Stargardt's disease/fundus flavimaculatus: psychophysical and electrophysiologic results. *Graefes Arch Clin Exp Ophthalmol.* 1993;231:555–562.
26. Lachapelle P, Little JM, Roy MS. The electroretinogram in Stargardt's disease and fundus flavimaculatus. *Doc Ophthalmol.* 1989;73:395–404.
27. Lois N, Holder GE, Fitzke FW, Plant C, Bird AC. Intrafamilial variation of phenotype in Stargardt macular dystrophy-fundus flavimaculatus. *Invest Ophthalmol Vis Sci.* 1999;40:2668–2675.
28. Moloney JB, Mooney DJ, O'Connor MA. Retinal function in Stargardt's disease and fundus flavimaculatus. *Am J Ophthalmol.* 1983;96:57–65.
29. Niemeyer G, Demant E. Cone and rod ERGs in degenerations of central retina. *Graefes Arch Clin Exp Ophthalmol.* 1983;220:201–208.
30. Fishman GA. Fundus flavimaculatus: a clinical classification. *Arch Ophthalmol.* 1976;94:2061–2067.

31. Stavrou P, Good PA, Misson GP, Kritzinger EE. Electrophysiological findings in Stargardt's-fundus flavimaculatus disease. *Eye.* 1998; 12:953–958.
32. Armstrong JD, Meyer D, Xu S, Elfervig JL. Long-term follow-up of Stargardt's disease and fundus flavimaculatus. *Ophthalmology.* 1998;105:448–457.
33. Cremers FP, van de Pol DJ, van Driel M, et al. Autosomal recessive retinitis pigmentosa and cone-rod dystrophy caused by splice site mutations in the Stargardt's disease gene ABCR. *Hum Mol Genet.* 1998;7:355–362.
34. Martinez MA, Paloma E, Allikmets R, et al. Retinitis pigmentosa caused by a homozygous mutation in the Stargardt disease gene ABCR. *Nat Genet.* 1998;18:11–12.
35. Maugeri A, van Driel MA, van de Pol DJ, et al. The 2588G→C mutation in the ABCR gene is a mild frequent founder mutation in the Western European population and allows the classification of ABCR mutations in patients with Stargardt disease. *Am J Hum Genet.* 1999;64:1024–1035.
36. Aaberg TM. Stargardt's disease and fundus flavimaculatus: evaluation of morphologic progression and intrafamilial co-existence. *Trans Am Ophthalmol Soc.* 1986;84:453–487.
37. Sun H, Molday RS, Nathans J. Retinal stimulates ATP hydrolysis by purified and reconstituted ABCR, the photoreceptor-specific ATP-binding cassette transporter responsible for Stargardt disease. *J Biol Chem.* 1999;274:8269–8281.
38. Weng J, Mata NL, Azarian SM, et al. Insights into the function of Rim protein in photoreceptors and etiology of Stargardt's disease from the phenotype in abcr knockout mice. *Cell.* 1999;98: 13–23.
39. Glenn AM, Fishman GA, Gilbert LD, Derlacki DJ. Effect of vitamin A treatment on the prolongation of dark adaptation in Stargardt's dystrophy. *Retina.* 1994;14:27–30.
40. Fishman GA, Farbman JS, Alexander KR. Delayed rod dark adaptation in patients with Stargardt's disease. *Ophthalmology.* 1991; 98:957–962.
41. Bush RA, Sieving PA. Inner retinal contributions to the primate photopic fast flicker electroretinogram. *J Opt Soc Am A.* 1996;13: 557–565.
42. Scholl HPN, Kremers J, Apfelstedt–Sylla E, Zrenner E. L- and M-cone driven ERGs are differently altered in Best's macular dystrophy. *Vision Res.* 2000;40:3159–3168.